

Effects of curing stress on the stiffness of a cement-mixed sand

Sérgio Filipe Veloso Marques^{1,*}, Nilo Cesar Consoli¹, and Lucas Festugato¹

¹Department of Civil Engineering, Universidade Federal do Rio Grande do Sul, Brasil

Abstract: Research into naturally cemented soils (e.g. sandstones) has increased considerably, mostly because of growing interest in offshore oil wells at depths that can, at times, exceed 1000 m. Performing tests directly with on-site soil samples is ideal. However, its acquisition, transportation and preservation are incredibly difficult. In order to perform the tests required for this study, the samples were made to simulate the bonding found in naturally cemented soils. Artificially cemented sands were cured under stresses of either 500, 2000 and 4000 kPa, or simply under atmospheric pressure. These specimens were then subjected to drained triaxial compression tests. The results have shown that the curing type has influence over the artificially cemented sand's yield surface and stiffness. The stiffness was vastly superior in specimens cured under higher levels of stress

1 Introduction

Few authors have investigated the effect of cement setting under stress in granular soils. The pioneering work was published by [1], who studied the behavior of artificially cemented samples cured under stress in oedometric tests. [2 - 10] verified the importance of considering curing stresses and curing void ratio in the mechanical behavior of cemented soils through isotropic and triaxial tests in an artificially cemented soil. These authors' results showed that values of the isotropic or anisotropic confining pressure during curing, have an influence on the stress-strain-dilatancy behavior of artificially cemented samples. To overcome the problem of the more frequent utilization of challenging soils regarding resistance and deformability for civil engineering works, the use of artificially cemented soils has served as a solution to make it suitable for use. The stress applied during curing in superficial improvements such as shallow foundations, make practically no difference, as this value is reduced. However, for applications at great depths (e.g. large landfills, offshore platforms, oil exploration wells, etc.), the stress function during curing has an influence on the stress-strain behavior of the artificially cemented soil.

[11] presented the first rational methodology that relates unconfined compressive strength (q_u) of clean granular soils treated with Portland cement with porosity/cement ratio (η/C_{iv}). This ratio, defined as the porosity (η) of the compacted mixture divided by the volumetric cement content (C_{iv}), takes into account both compaction and cementation amount. This means that the designer can choose to apply higher compaction energy or add more quantity of cement to reach a specific

value of strength. Same dosage methodology was extended to tensile strength (q_t) [12] and initial shear modulus [13].

2 Materials, sample preparation and testing procedure

The material used in this testing is a sand from a region of Osorio near Porto Alegre in southern Brazil. It was classified [14] as non-plastic uniform fine sand (SP) and the specific gravity of the solids is 2.65. Mineralogical analysis showed that sand particles are mainly quartz. The grain-size distribution is entirely fine sand with a mean diameter (D_{50}) of 0.20 mm and the uniformity and curvature coefficients of 2.11 and 1.15, respectively. The minimum and maximum void ratios are 0.60 and 0.90, respectively. Early strength Portland cement (Type III) was chosen as the cementing agent due its rapid gain on strength, which allowed for establishing three days as the curing time. The specific gravity of the cement is 3.15. Distilled water was used in the molding process.

The triaxial tests series were performed with uncemented and cemented soil specimens cured under stress or under atmospheric pressure. The specimens of cemented soil were prepared by initially mixing quantities of dry soil with powdered Portland cement. Secondly, water was added to the mixture, making sure that proper homogeneity was obtained by mixing. The soil-cement mixture was statically compacted at specified density in three layers into a cylindrical mold (50 mm diameter x 100 mm high). Immediately after extraction from the mold, the specimen was weighed with an accuracy of 0.01 g and had its diameter and height measured

* Corresponding author: smarques@ufrgs.br

with an accuracy of 0.1 mm. When cured under atmospheric pressure, the specimens were placed into plastic bags to avoid significant variations in moisture content and left to cure in a temperature-controlled room ($23^{\circ} \pm 2^{\circ}C$). When cured under stress, the specimen was placed in the triaxial chamber and then consolidated under different confining stress levels ($p' = 500, 2000$ or 4000 kPa), at a rate of 500 kPa/min. The time for both curing methods before triaxial shearing under different confining stress (500, 2000 or 4000 kPa) was 72h.

It was chosen three cement content and a specific void ratio in the order to get three different η/C_{iv} (10, 17 and 30), based on previous studies by [15 and 13]. In order to perform a correct comparison between the cemented samples, it was defined that specimens should be cured with the same η/C_{iv} . Specimens cured under atmospheric pressure were directly molded in the η/C_{iv} predefined (η/C_{iv} after molded, Table 1). The specimens cured under stress were molded with η/C_{iv} (higher void ratio) in such a way that they would reach the requisite values for curing after consolidation (η/C_{iv} at the start of shearing, Table 1). This method allowed all specimens to be cured, under stress or under atmospheric pressure, with the same η/C_{iv} . Due to the difficulty of obtaining the exact η/C_{iv} required, it was defined that the specimens should be within a range of the required $\eta/C_{iv} \pm 0.5$ to be considered acceptable.

After the curing process, the specimens were submitted firstly to saturation. A simultaneous raising of both cell pressure and back pressure, keeping the effective stress constant, accomplished this step. Parameter B values were not measured to avoid damaging the bonds within specimens [16]. After that process, an axial load, under a drained condition, was carried out using controlled deformation at a displacement rate of 1 mm/h. The shear test, for the samples cured under stress, were performed with the same effective stress they were cured.

Hall effect sensors [17], one radial and two axial, were used to measure the internal displacement with a resolution smaller than 1 μm . An LVDT, with a resolution smaller than 10 μm , was used to measure the relative displacement between the triaxial chamber and the loading piston. All the triaxial tests followed the general procedures described by [18] and the area corrections proposed by [19] were adopted to calculate the applied stresses. All performed tests are listed in Table 1.

To identify the tests, the following nomenclature $a(b)c-d$ was used, where a is the type of curing process (ATM = Atmospheric Pressure; US = Under Stress), b is the η/C_{iv} which each specimen was cured, c is the effective curing stress and d is the effective stress during shearing.

3 Test Results and Analysis

The stress-strain response during the drained shearing compression test for specimens were similar. For both curing cases, the response to the shearing at lower effective stress presents a softening following a peak. To other levels of effective stress, the results showed a

Table 1. Summary of the drained triaxial compression tests.

Specimen	Curing Stress (kPa)	Effective stress during shear (kPa)	% Cement	Void Ratio after molded	η/C_{iv} after molded	Void ratio after curing	Void Ratio start shearing	η/C_{iv} start shearing	q_{max} (kPa)	$q_{plastic}$ (kPa)	$q_{residual}$ (kPa)	q_u (kPa)	G_{max} (kPa)	a	b
SAND(17*0-500)	0	500	0	0,68	-	-	0,67	-	1437	356	1326	-	-	-	-
SAND(17*0-2000)	0	2000	0	0,68	-	-	0,65	-	4789	1022	4789	-	-	-	-
SAND(17*0-4000)	0	4000	0	0,72	-	-	0,68	-	8486	1424	8482	-	-	-	-
ATM(170-500)	0	500	4,71	0,66	17,2	-	0,65	17,0	1966	570	1537	676	300	3,886	1,016
ATM(170-2000)	0	2000	4,71	0,64	16,8	-	0,62	16,3	5223	1143	5016	698	660	3,287	1,046
ATM(170-4000)	0	4000	4,71	0,62	16,5	-	0,59	15,6	9342	1452	9337	724	1200	3,868	0,994
US(10)500-500	500	500	8,35	0,70	10,6	0,68	0,68	10,4	2498	680	2041	1299	1200	13,736	1,072
US(10)2000-2000	2000	2000	8,35	0,68	10,3	0,65	0,65	9,8	5946	1920	5755	1395	1500	7,469	1,012
US(10)4000-4000	4000	4000	8,35	0,70	10,7	0,65	0,65	9,9	10741	3774	10240	1377	1800	5,930	0,922
US(17)500-500	500	500	4,71	0,68	17,7	0,66	0,66	17,4	2089	619	1601	667	750	9,869	1,060
US(17)2000-2000	2000	2000	4,71	0,67	17,5	0,64	0,64	16,7	5250	1779	5225	706	1000	5,204	1,044
US(17)4000-4000	4000	4000	4,71	0,68	17,8	0,63	0,63	16,7	9522	2756	9510	707	2000	8,116	0,920
US(30)500-500	500	500	2,5	0,66	30,7	0,64	0,64	29,9	1687	461	1376	332	600	10,240	1,024
US(30)2000-2000	2000	2000	2,5	0,70	32,8	0,65	0,65	30,3	4854	1402	4854	326	800	5,267	0,965
US(30)4000-4000	4000	4000	2,5	0,71	32,3	0,67	0,67	30,2	8480	2402	8480	315	1175	6,297	0,921

Note: * moulded with a equivalent void ratio of specimens US(17)

hardening behavior. In terms of maximum deviatoric stress, the results are quite similar (see Table 1) between both types of tests, with different curing processes, and

for all effective stress levels. While the increases in effective stress cause a more compressive response in volumetric strain, the specimens cured under stress present a more expansive when compared to the specimens cured under atmospheric pressure. Stress-strain behaviors, changes from peak softening to a non-peak response in terms of stress-strain and changes to volumetric behavior according to effective stress are well documented in the literature [2, 20 - 23]. The main difference between the utilized curing methods is that specimens cured under stress have an increased stiffness and a less contractive response in volumetric terms. Fig. 1 shows the stress and variation of the secant stiffness with the shear strain of the cemented specimens cured by different methods, and an uncemented specimen with a void ratio similar to the cemented mixtures, only for comparison. To calculate the secant stiffness (G_{sec}), Eq. 1 was used.

$$G_{sec} = \frac{q}{3\epsilon_s} \quad (1)$$

where q is the deviator stress, and ϵ_s is the shear strain.

It was performed a test in an equivalent void ratio sand for comparison only. The results show a higher stiffness for the cemented specimens cured under stress followed by the cemented specimens cured under atmospheric pressure. These results, also found by other authors (e.g. [2, 6, 7, 8]) to curing stress under 500 kPa, indicates that the preservation of the structure of the specimen, when cured under stress, increase significantly the stiffness in shearing. Fig. 1b shows the comparison of the stiffness for the specimens sheared at a constant effective stress of 500 kPa. Since it is impossible to analyze the integrity of the specimens just before shearing, it is assumed that stiffness loss for the specimen cured under atmospheric pressure is due to the effective isotropic pressure application after the curing process, that possibly caused a series of cement bonds breakage (cracks) in the specimen. Using a scanning electron microscope, [24] observed cracks in specimens that passed by an unloading process after being cured under stress.

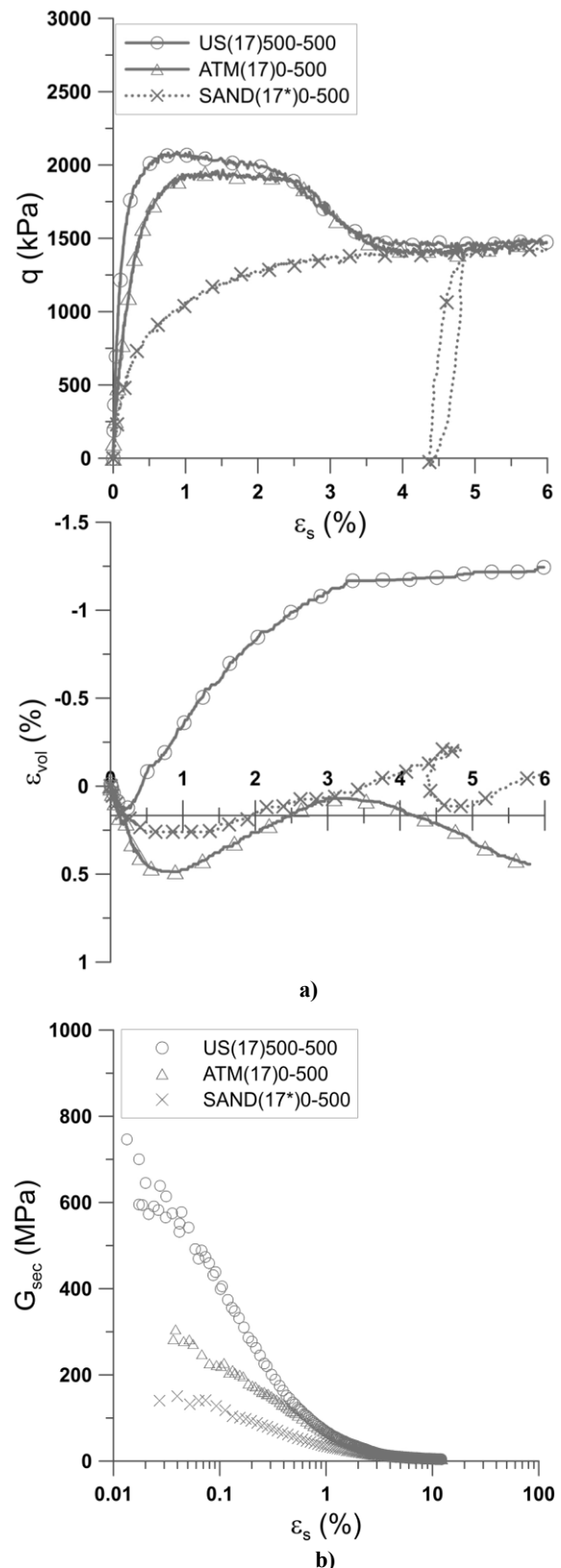


Fig. 1. Behavior of uncemented (SAND), cemented cured under stress (US) and under atmospheric pressure (ATM) specimens: a) deviatoric stress-volumetric-shear strain and b) secant stiffness-shear strain.

As shear stresses increase or decrease materials distort, i.e., change shape. The relationship between shear stress and shear strain it is the shear modulus G . Stiffness variation analysis can be performed in terms of secant shear modulus (G_{sec}) versus distortional strain (ϵ_s) in a logarithmic scale. The S-shaped curve is typically obtained from dynamic (e.g.: bender element or resonant column tests) and monotonic tests (e.g. triaxial compression test). The measurement of shear modulus at very low strain (G_{max}) in triaxial are usually obtained by dynamic methods (e.g. bender elements technique) and local strain measurement. Due to technical impossibilities, bender elements measurements were not performed for this work. By this constraint, G_{max} was estimate using $G_{sec}:\epsilon_s$ curves, which were obtained by local strain measurement (hall effect sensor system coupled to the sample) and mathematical models present in bibliography.

Several authors [25, 26, 27] have proposed simple and empirical models described by a parabolic equation to fit the evolution of shear modulus with distortion strain. In order to achieve a better adjustment, a combination of the models of the above-cited authors was proposed which resulted the Eq. 2.

$$G = \frac{G_{max}}{1+a(\epsilon_s)^b} \quad (2)$$

Least squares method was used to adjust the proposed equation (Eq. (2)) to the triaxial tests results of this study allowing to estimate the G_{max} values and to determine the empirical parameters a and b for each test. Fig.2a shows the application of Eq. 2 to $G_{sec}:\epsilon_s$ curves of the tests ATM(17)0-4000 and US(30)2000-2000. A good fit ($R^2 > 0.996$) is evident between the G_{sec} results and the proposed model. All tests presented a determination coefficient (R^2) higher than 0.99. The G_{max} value and the a and b parameters for each test are listed in table 1. For the certification that the suggested G_{max} value was adequate, the model fit was also verified in the stress-strain space ($q:\epsilon_s$), which, as shown in Figure 2b, presents a reasonable relationship.

4 Discussions and Conclusions

The result of triaxial tests of cemented materials cured under stress has demonstrated the importance of that curing methodology in the study of cemented materials, mainly when it comes to the stiffness and dilatancy behavior. The test results indicate that the maximum shear stress is very similar for both types of cure, but has a considerable difference in the stiffness for small strains and the yield loci. Bond degradation occurs during the isotropic consolidation of the cured samples under atmospheric pressure. The main contribution of this work is to show the necessity of the under-stress curing method to truly study the behavior of this type of artificially cemented soil or to simulate naturally cemented soils. This will significantly influence the characteristics of the constitutive models required to simulate these soils.

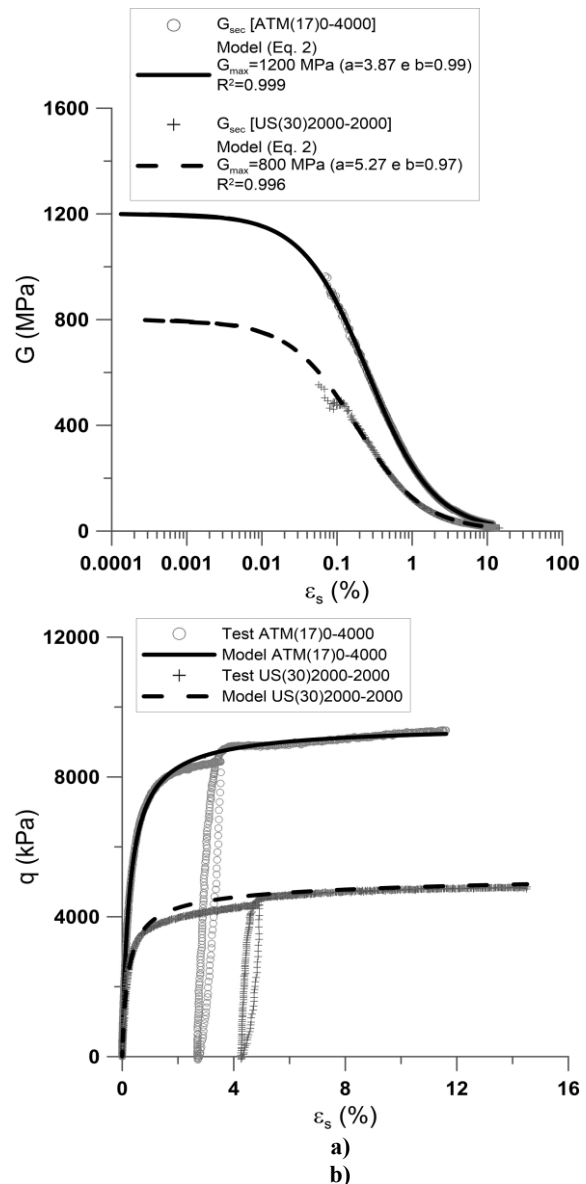


Fig.2. a) Model fit for the G_{sec} results of tests in space $G:\epsilon_s$ and b) Adjustment of the model to the stress-strain curve of tests in the space $q:\epsilon_s$.

References

1. F. Zhu, J. Clark, M. Paulin, *Can. Geotech. J.*, **32**, 195-203 (1995)
2. N. C. Consoli, G. V. Rotta, P. D. M. Prietto, *Géotechnique*, **50**, 1, 99-105 (2000)
3. N. Consoli, G. Rotta, P. Prietto, *Géotechnique*, **56**, 69-72 (2006)
4. N. C. Consoli, D. Foppa, L. Festugato, K. S. Heineck, *J. of Geotech. and Geoenv. Eng.*, **133**, 2, 197-205 (2007)
5. G. V. Rotta, N. C. Consoli, P. D. M. Prietto, M. R. Coop, J. Graham, *Géotechnique*, **53**, 5, 493-501 (2003)
6. H. Ahnberg, *Can. Geotech. J.*, **44**, 54-66 (2007)
7. F. Dalla Rosa, N. C. Consoli, B. A. Baudet, *Géotechnique*, 675-679 (2008)
8. A. Rabbi, J. Kuwano, J. Deng, T. Boon, *Soils and Found.*, 651-661 (2011)

9. M. Suzuki, T. Fujimoto, T. Taguchi, *Soils and Found.*, 687-698 (2014)
10. R. Zhang, J. Zheng, X. Bian, *Acta Geotechnica*, **12**, 921-936 (2017)
11. N. C. Consoli, L. S. Lopes Junior, K. S. Heineck, *J. of Mat. in Civ. Eng.*, **21**, 5, 210-216 (2009)
12. N. C. Consoli, R. C. Cruz, M. F. Floss, L. Festugato, *J. of Geotech. and Geoenv. Eng.*, 759-763 (2010)
13. N. C. Consoli, R. Cruz, A. Viana da Fonseca, M. Coop, *J. of Geotech. and Geoenv. Eng.*, **138**, 1, 100-109 (2012)
14. ASTM. D2487: Standard Practice for Classification of Soils for Engineering Purposes (Unified Soil Classification System). West Conshohocken, PA, USA: ASTM International (2011)
15. N. C. Consoli, A. Viana da Fonseca, R. C. Cruz, K. S. Heineck, *J. of Geotech. and Geoenv. Eng.*, **9**, 1347-1353 (2009)
16. L. Bressani, P. Vaughan, Damage to soil during triaxial testing. 12nd Int. Conf. On Soil Mechanics and Foundation Engineering, 533-552, Rio Janeiro: A. A. Balkema. (1989)
17. C. R. I. Clayton, S. Khatrush, A. Bica, A. Siddique, *Geotech. Testing. J.*, **12**, 1, 69-76 (1989)
18. ASTM. D7181-11: Method for Consolidated Drained Triaxial Compression Test for Soils. West Conshohocken, PA, USA: ASTM International (2011)
19. P. La Rochelle, S. Leroueil, B. Trak, Blais-Leroux, F. Tavenas, Observational approach to membrane and area correction in triaxial tests. Symposium on advanced triaxial testing of soil and rock. Louisville: Proceedings: American Societ of Testing and Materials (1988)
20. G. Elliot, E. T. Brown, *Géotechnique*, **35**, 4, 413-423 (1985)
21. M. Coop, J. Atkinson, *Géotechnique*, **43**, 1, 53-67 (1993)
22. T. Cuccovillo, M. Coop, *Géotechnique*, **49**, 6, 741-760 (1999)
23. A. Marri, D. Wanatowski, H. S. Yu, *Geomech. and Geoeng.: An Int. J.*, 1-16 (2012)
24. G. Alvarado, M. Coop, S. Willson, *Géotechnique*, **62**, 4, 303-316 (2012)
25. B. Hardin, V. Drnevich, *J. of the Soil Mech. and Found. Div.*, 667-692 (1972)
26. J. Santos, A. Correia, Reference threshold shear strain of soil. Its application to obtain a uique strain-dependent shear modulus curve soil. 15th Int. Conf. SMGE, **1**, 267-270. Istambul: A.A. Balkema (2001)
27. K. Stokoe, M. Darandeli, R. Gilbert, F. Menq, W. Choi, Development of a new family of normalized modulus reduction and material damping curves. International Workshop on Uncertainties in Nonlinear Soil Properties and their Impact on Modeling Dynamic Soil Response. UC Berkeley (2004)